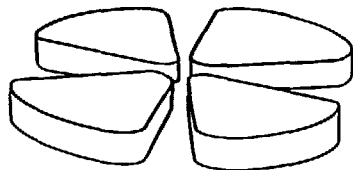


9100687

GANIL



HOT NUCLEI STUDIED WITH HIGH EFFICIENCY
NEUTRON DETECTORS

J.Galin

GANIL BP 5027, 14021 Caen-Cedex, France

XXIST Summer School on Nuclear Physics MIKOLAJKI (Poland)

(Aug 26-Sept 5 1990)

To be published by IOP Publishing Limited

GANIL P 90 17

HOT NUCLEI STUDIED WITH HIGH EFFICIENCY NEUTRON DETECTORS

J.Galin

GANIL BP 5027, 14021 Caen-Cedex, France

1. INTRODUCTION

It is a long time since nuclear physicists and astrophysicists became interested in hot nuclei but it is only recently that experimental studies have been undertaken. With the advent of intermediate energy heavy ion beams, hot nuclei can be formed with large cross sections and this facilitates their investigation.

How can we define a hot nucleus? First, when we consider nuclei, this implies ensembles of nucleons which remain selfbound systems, at least for some time. Second, to apply the concept of temperature to such objects, they must be in thermal equilibrium. How far can we extend the concept of hot nuclei? This is a difficult question that confronts experimentalists and theorists. Theorists have approached the problem from both a static and a dynamic point of view. Experimentalists have tried to prepare hot nuclei with given conditions of mass, isospin, temperature, compression, etc. and to characterize their properties by studying their decay.

After the pioneering work of Brack and Quentin (1974), temperature dependent Hartree-Fock calculations and Thomas-Fermi calculations have been performed by Bonche et al (1984, 1985) and Suraud (1987) respectively, showing that above a certain temperature a nucleus does not remain a selfbound system. Not surprisingly the Coulomb energy is shown to have an important disruptive effect: a fictitious uncharged nucleus or a very neutron-rich nucleus can sustain larger temperatures than actual nuclei. Similarly, a light nucleus can be more heated than a heavy one before disintegrating. However, one should exercise caution in comparing these theoretical limits with those that can be inferred experimentally. Indeed such theories, being

equilibrium theories, are not concerned with the mechanism by which the nucleus has been heated up. In particular, they do not take into account the fact that in addition to the disordered energy (heat), some collective energy (rotational, compressional energies) can also be given to the nucleus, especially when it is born from a nucleus-nucleus collision. Different approaches by Nemeth et al (1986), Vinet et al (1986, 1987), Vautherin et al (1987) have shown that compression energy can be as effective as thermal energy to destabilize the nucleus.

Time dependent microscopic calculations currently provide the most complete model for the dynamics of the collision. When the hot nuclei are formed with projectiles of several tens of MeV/u, there is a strong interplay between the effects of the self consistent mean field and the individual nucleonic collisions. These effects can be taken into account in semi-classical approaches which have shown the influence of the different parameters of the collision (impact parameter, projectile velocity, size of the nuclei, etc) on dissipated energy (thermal and collective), relaxation time, etc. When formed in a nucleus-nucleus collision, a hot nucleus is a very elusive object which becomes more and more difficult to define when its temperature increases. As shown by Delagrange et al (1986), above $T=5$ MeV, the estimated decay time through particle evaporation becomes smaller than the characteristic relaxation time. This could introduce some kind of dynamic limitation in the observed temperatures which has nothing to do with the static limits considered previously.

After all these considerations it can be easily guessed that if the task of the theorist to integrate both dynamic and static effects in a unique approach is most difficult, the task of the experimentalist is not easy, either. Progress cannot be made from a single experiment but must come from many different approaches. First, one has to investigate the different ways to heat up a nucleus. What is the influence of impact parameter, projectile energy, size of interacting nuclei, their isospin, etc, on the dissipated energy? How can one infer this energy from current observables? Are some observables better than others? What are the most appropriate tools? The measurement of this energy (or alternatively the temperature) has been the purpose of many efforts in the past and different kinds of "thermometers" have been proposed. Amongst them, light particle (either charged or neutral) multiplicity measurements play an important role. This is because, as opposed to other approaches, they do not require an a priori knowledge of the decay modes (fission, multiple fragmentation, sequential or not) that the nucleus or the nuclear system can undergo, and thus, are more generally applicable.

During these lectures we would like to present some examples of what has been_ and could be_ done when exploring different kinds of reactions. Since the information that can be gained depends strongly upon the observables, it is worth devoting the second part of the lecture to

experimental problems and more specifically to neutron detection. Then, we will review the information that has been derived from inclusive neutron multiplicity measurements. In the fourth section attention will be paid to peripheral collisions and it will be shown that fairly excited nuclei can be formed in some of them. In the fifth section, dissipative collisions will be considered in some detail and finally we will summarize.

2. NEUTRON MULTIPLICITY METERS

Four-pi, high efficiency neutron detection appears to be a very powerful and promising method to study, not only the formation and decay of hot nuclei, but also, reaction mechanisms, more generally. It is thus worth considering some experimental aspects in details.

2.1 Basic principle of 4π neutron multiplicity meters

Gadolinium loaded, liquid scintillator neutron detectors were invented by Reines et al (1954) to provide high efficiency detection and numbering of neutrons emitted in a single nuclear reaction, as also illustrated by Frehaut (1976). Such detectors were revived by Cheifetz et al (1972) during the quest for super-heavy elements, whose fission was expected to free an unusually large number of neutrons. More recently, they have been utilized by Jahnke et al (1983) and Schroeder et al (1988) to study heavy-ion reactions at low energy.

Let us first recall the basic principle of gadolinium loaded, liquid scintillator detectors. They are made of a solvent, two scintillating components and a gadolinium salt. As schematized in

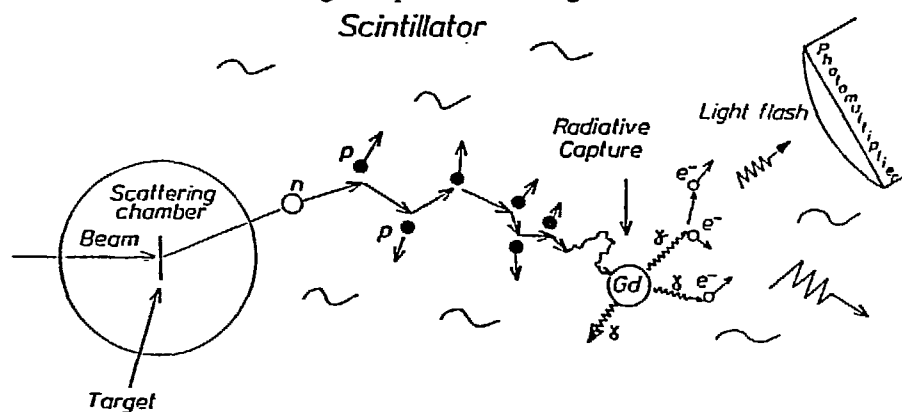


Fig.1 Scheme for neutron detection in Gd loaded, liquid scintillator detectors.

Fig.1, neutrons are slowed down by elastic scattering on the H and C nuclei of the organic medium till thermalization. Thereafter, they wander for about 10 μ s before being captured by gadolinium nuclei or, less frequently, by hydrogen or carbon. Indeed, gadolinium has huge neutron capture cross sections as compared to H and C. The emitted gamma-rays, three on the average, are then detected by a bunch of photomultipliers surrounding the scintillator tank. Due to the time delay and time spreading between neutron emission and detection, the neutrons emitted in a single nuclear reactions can thus be easily numbered. The most interesting property of such a detector is its high efficiency, typically 85-90% for 2 MeV neutrons.

2.2 The ORION detector

In order to efficiently utilize its 3 m³ of scintillator, the 4 π detector ORION, in operation at GANIL for two years, has been designed with the beam axis as symmetry axis and a larger quantity of scintillator forward than backward (Fig.2). This is required to optimize the detection of neutrons with more energy, and thus with a larger mean free path, forward than backward. The scattering chamber is embedded in the scintillator tanks to ensure 4 π detection. The

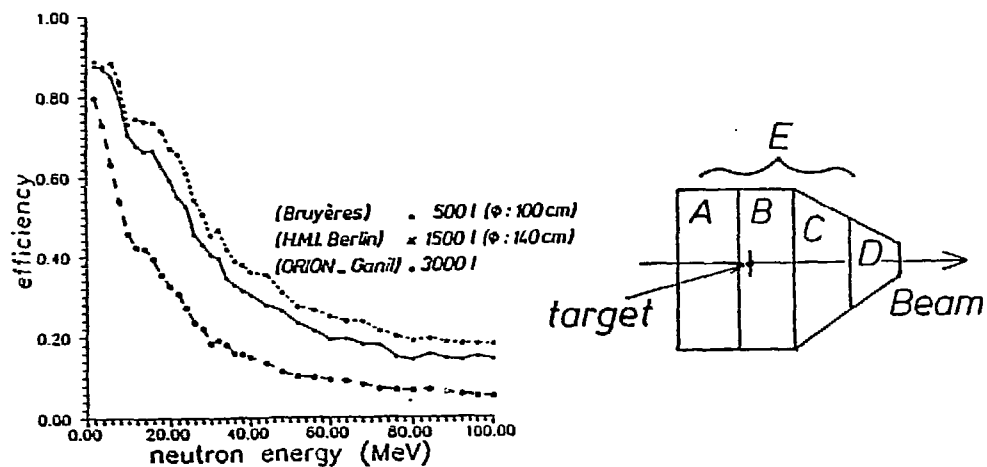


Fig.2 Detection efficiency computed as a function of kinetic energy for neutrons emitted isotropically in three detectors used at GANIL. The geometry of ORION is also schematized.

detector efficiency can be computed by a Monte-Carlo method, developed by Poitou et al (1974) and recently updated by Prot and Wang (1989) to take account of the geometry of ORION and to extend the neutron energy range up to 100 MeV. The detector efficiency is shown, in Fig.2, as a function of neutron kinetic energy, with neutrons assumed to be distributed isotropically from a point source. The efficiency remains essentially constant (close to 90%) up to 6 MeV where a fall off appears. This is due to the onset of the C(n, α)Be channel in which the neutron gets lost. Above 18 MeV, the growing influence of the C(n,p)B reaction is mainly responsible for the continuous loss in efficiency. Therefore, even with an infinite size detector, the detection efficiency would remain low for energetic neutrons when using gadolinium loaded type detectors. As we will see later on, one can take advantage of this selectivity in energy to retain neutrons of evaporative origin and disregard those emitted in the first steps of a reaction, prior to equilibrium, and thus, much faster.

Details about the in-beam operation of such a detector have been presented elsewhere by Galin et al (1990). Here, we would like to show the new information that can be gained from the sectorization of ORION. Indeed, counting the neutrons in each sector separately provides interesting information on the spatial distribution of these neutrons and, hence, gives clues

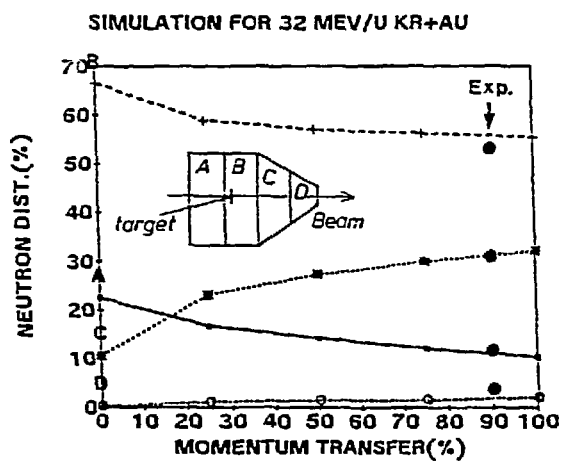


Fig.3 Sharing of neutrons registered in the 4 sectors of ORION, as simulated for different momentum transfers (0%, 25%, 50%, 75%, 100%). Experimental data for Cf match the computed ones at 0% momentum transfer. The Kr+Au experimental data, selected for events with 30-35 detected neutrons, are shown by solid dots.

as to their origin. This can be simply shown as follows. First, let us consider the simple case of a Cf source installed at the target spot and emitting neutrons, whose properties are perfectly known. Simulated data reveal a perfect agreement with experimental ones, and the differences in partial multiplicities observed in the sectors, for isotropically emitted neutrons, show nothing but the differences in detection solid angles (Fig.3). Then, the nuclear reaction, 32 MeV/u Kr on Au, has been considered, with selection of events characterized by a very large neutron multiplicity (30-35). The distribution of these neutrons amongst the four sectors of ORION reveals, as shown in Fig.3, a very strong focusing as expected when emission occurs from a forward recoiling source. Simulations have then been performed assuming pure statistical evaporation from a single source whose velocity depends on initial momentum transferred from projectile to the fused system. Details on the simulation have been presented elsewhere, by Galin et al (1990), and we only give in Fig.3 the results. It is shown that, in reasonable agreement with data from Bougault et al (1990) and Pollaco et al (1990), a large momentum transfer, close to 90% of the projectile momentum, is required to best reproduce the considered experimental data. It is also shown that preequilibrium neutrons, necessarily very few since 90% of momentum transfer has been reached, hardly show up in excess of predicted evaporated ones in the most forward sector D (it must be also reminded that detection efficiency drops down for high energy, direct emission).

These two examples have demonstrated the feasibility for extracting very valuable spatial information from the neutrons when utilizing a sectorized detector. However, it must be emphasized that, due to cross-talk between adjacent sectors (about 20% in the present configuration), the granularity of this type of detector can not be very much improved. In this respect, 4π charged particle detectors do not suffer the same limitation.

2.3 Some prospects on global kinetic energy measurements

In addition to the multiplicity information, brought in by thermal neutron captures, this detector provides, as non-loaded plastic scintillators do, a prompt signal, strongly connected with the neutron multiplicity. Within several tens of ns after the nuclear reaction, i.e., well before neutron capture has occurred, a light signal is generated by both prompt gamma-rays and recoiling protons, following neutron scattering. Although slightly separated in time, these two components cannot be resolved. However, due to the large neutron multiplicities accompanying the reactions we are mostly interested in, it is expected that light originates essentially from the neutrons. This is well shown in Fig.4, where a strong correlation can be observed between the

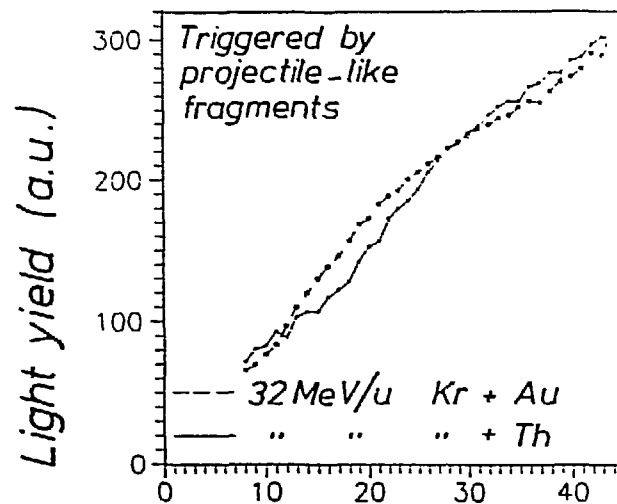


Fig.4 Total light yield, measured in ORION, as a function of detected neutron multiplicity.

prompt light yield signal and neutron multiplicity. To exploit further this information, in each sector separately, one has to take into account, in addition to the number of neutrons hitting a given sector, the kinetic energy of these neutrons. This can be achieved through a Monte-Carlo simulation after having assumed some model for neutron emission. Progress is being made along these lines and it is expected that this will provide additional experimental constraints when testing the origin of detected neutrons.

2.4 Neutron multiplicity meters used as impact parameter filters

In order to illustrate the role that 4π neutron detectors can play as filters on impact parameter, let us consider some preliminary data obtained by Piasecki et al (1990) when bombarding a Au target with a 29 MeV/u Pb beam. A charged particle detection array, set in the forward direction and extending from the grazing angle to 11° beyond it, has allowed us to probe a large fraction of the reaction products with Z's ranging from Z=4 to Z=82. As it can be guessed, for such a massive system, all lines of Z's are populated when viewed in a standard dE-E identification matrix (Fig.5). The use of a multiplicity filter can shed light on the origin of the observed products. For a gate on neutron multiplicity set at (0-10), one observes a spike in the ID matrix,

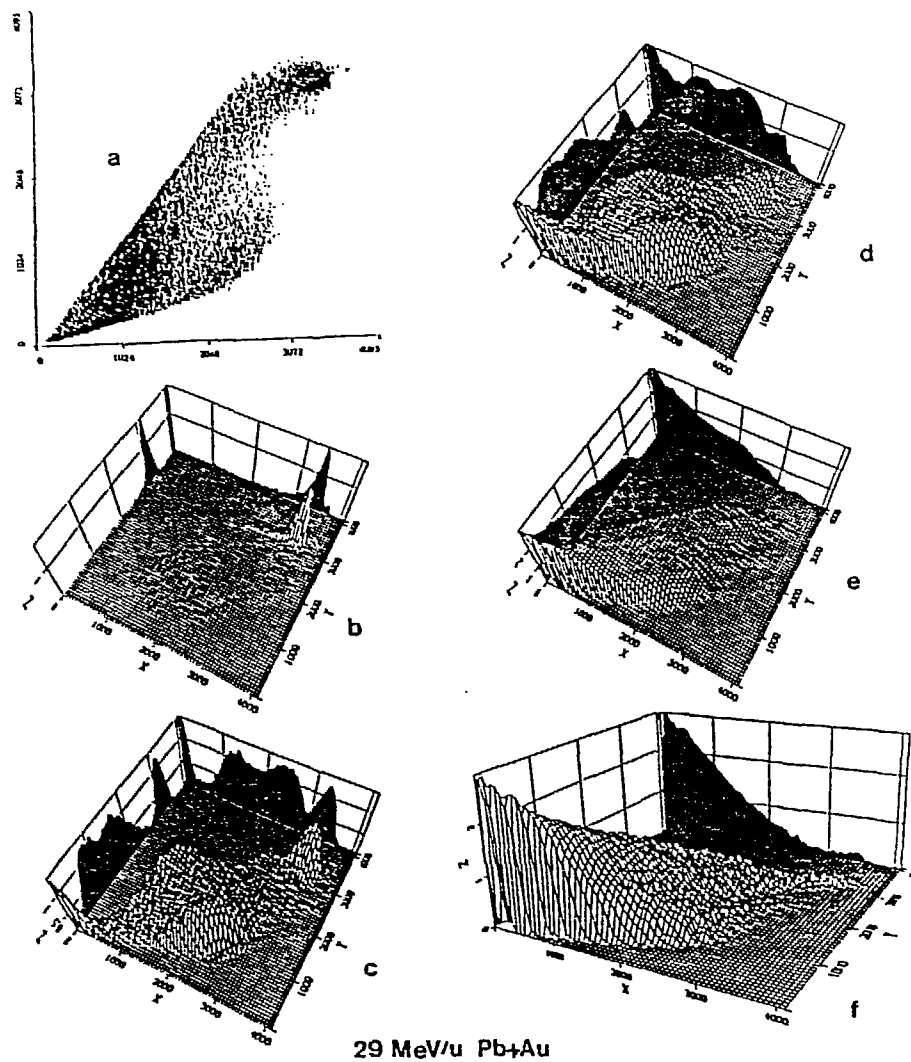


Fig.5 a) DE-E identification matrix as observed close to the grazing angle, ungated
 b) Contours in the DE-E space, gated on neutron multiplicities from 1 to 10
 c) Same as b with 11-20 neutrons
 d) Same as b with 21-30 neutrons
 e) Same as b with 31-40 neutrons
 f) Same as b with 41-60 neutrons

corresponding mostly to elastically scattered Pb. For the next multiplicity gate (11-20), the topography is strongly modified: the elastic spike has been replaced by a smoother hill which spreads in both Z and E, as expected for more and more inelastic events. In addition to these projectile-like fragments, some others, excited enough to undergo fission, are observed with Z's of roughly half the projectile Z. These fission fragments appear in two well separated bumps of different energies, as expected when the recoil velocity of the fissioning nucleus exceeds the center of mass velocity of the fragments. For the next multiplicity gate (21-30), the projectile-like nucleus undergoes still more damping and hence becomes more and more fissile. Only a few of them, the lightest, and presumably the less excited, can avoid fission. At the same time, a strong population of the so called Intermediate Mass Fragments (IMF extending from the lightest fission fragments down to alpha-particles) shows up. The emission probability of such fragments has been observed by Jiang et al (1988) and Sokolov et al (1990) to depend strongly on excitation energy. This IMF emission becomes dominant when triggered by the highest multiplicity gates (31-40) and (41-60). Simultaneously, both projectile-like fragments or their fission products disappear. The nuclear system explodes in a large number of neutrons_ about 80 after efficiency correction_ and IMF. The neutron number, by itself, represents one third of the total number of neutrons contained into the interacting nuclei. There are also, most likely, a large number of neutrons bound to one or two protons to form hydrogen and helium isotopes in such a way that about one half of the neutrons of the whole system might appear as relatively light particles and the rest, essentially in IMF. From these preliminary data there are thus strong clues that the nuclear system Pb+Au has disintegrated into fairly small nuclear pieces. This phenomenon represents roughly one fourth of the reaction cross section and is thought to appear in the most central collisions. Whatever the way this disintegration proceeds, in sequence or simultaneously, this result is all the more surprising since the bombarding energy is less than 15 MeV/u in the center of mass system. Is it the very strong Coulomb interaction for such a massive complex that favors its disassembly?

Through this example, we have demonstrated the capacity of 4π neutron detectors, first, in their role of filter on the impact parameter, then, as meters: when so many neutrons are freed from a nuclear system, they have to be numbered!

2.5 The coupling of ORION with 4π charged particle detectors

The previous example has naturally brought us to the coupling of 4π neutron detectors with 4π charged particle detectors. Is this coupling possible and how? The perturbation caused on the

neutron detection by an inner shell of charged particle detectors depends strongly on the characteristics of the latter. If one considers thin transmission detectors, made of silicon or plastic, the perturbation will be minor but the information on charged particles will be essentially reduced to their multiplicity. If one tries to improve the response of the particle detectors (identification, energy), by thickening them (stop detector), then more and more neutrons will suffer scattering before entering the liquid scintillator tanks and their angular distribution will be smeared. Low energy neutrons can even be lost. A compromise needs to be made: the more we want to learn about the charged particles, the less information will become available from the neutrons. The coupling of ORION with INDRA, a high standard 4π detector presently under construction at GANIL is foreseen. The housing of INDRA into ORION will require an enlargement of ORION.

3. INCLUSIVE DATA

3.1 General features

Inclusive neutron multiplicity distributions are easy to measure and have been extended over a broad range of projectile-target combinations and bombarding energies. They provide information on the energy dissipation capacity of a reaction, which is otherwise hardly

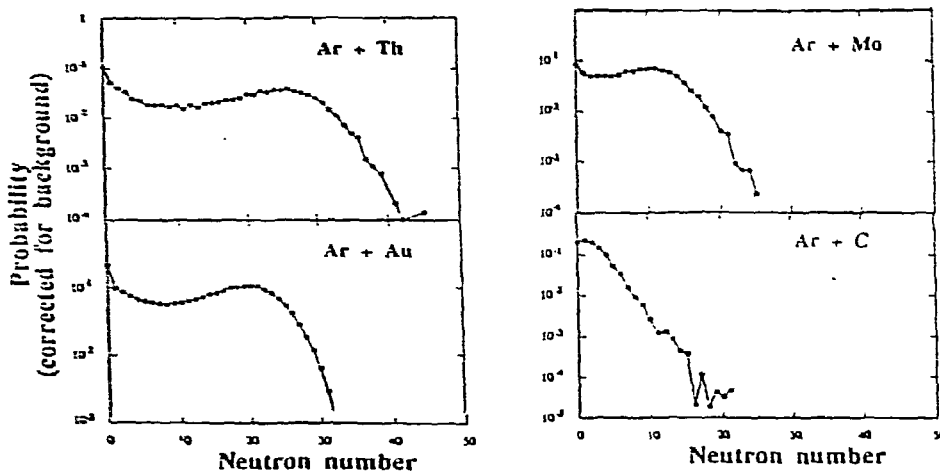


Fig.6 Neutron multiplicity distributions as measured (no efficiency correction) with an Ar beam at 44 MeV/u impinging on different targets.

accessible. Examples of such distributions obtained by Sokolov et al (1990), are given in Fig.6 for Ar reactions induced at 44 MeV/u on a series of targets. All types of nuclear reactions are registered according to the number of neutrons with a probability which can be converted in absolute cross sections.

The sum of the partial cross sections over all neutron numbers is in agreement, within 20%, with what is expected for the reaction cross sections, following Wilcke et al (1980). The spectra exhibit two distinct components: a gaussian shape bump at high multiplicity, originating mostly from central collisions and another component, decreasing from low neutron multiplicities, associated with peripheral collisions. The large number of neutrons that are measured from the heavy targets reflects nothing but the capacity for a heavy nucleus to evaporate more neutrons than charged particles, a phenomenon well known at low excitation energies. This effect is also accentuated by the fact that recoil velocity of the fused systems is smaller for heavy targets and, hence, evaporated neutrons, less boosted, are more efficiently detected.

It is obvious from the above considerations that 4π detectors are more sensitive, and thus better suited, for investigating heavy systems than light ones. This is even better illustrated when considering, in Fig.7, inclusive multiplicity data, by Piasecki et al (1990), on the Pb+Au system, one of the heaviest systems studied with the 4π neutron detector. The overall pattern

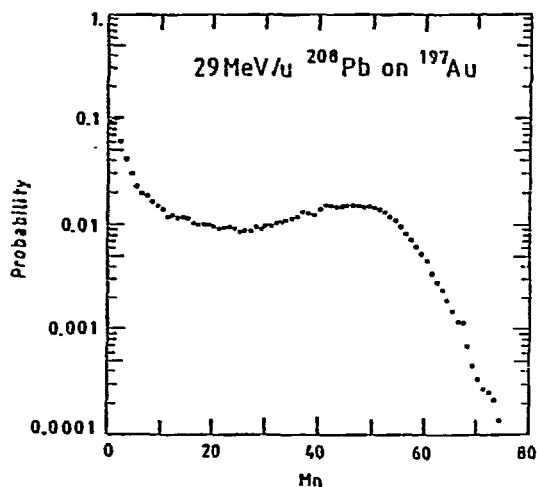


Fig.7 Neutron multiplicity distribution for 29 MeV/u Pb+Au, as obtained without efficiency correction.

resembles very much the ones shown previously in Fig.6, but it extends over a much broader range of neutron multiplicities. As it could already be shown in Sec.2.4, one possesses, with this multiplicity observable, a very powerful tool to select reactions according to their impact parameter.

3.2. Neutron multiplicity and energy dissipation

Gross information on energy dissipation can be carried out from very simple neutron multiplicity measurements in so far as heavy systems are considered. This is simply because neutron evaporation is then strongly dominant, as shown by Jiang et al (1989), and neutrons alone can provide a reliable picture on energy dissipation. Moreover, the 4π detector having a good efficiency for low energy neutrons _ typically, those evaporated from a slow moving target-like source_ and a very poor efficiency for high energy neutrons _typically, those emitted either by a fast moving and light projectile-like nucleus or at a preequilibrium stage_ operates a natural selection to retain those neutrons of greatest interest in so far as energy dissipation is considered.

Two series of measurements have been performed in order to determine the most efficient way for degrading kinetic energy into heat in a nuclear system. First, for a given nuclear system (Ar+Au), the effect of bombarding energy has been investigated in modifying the beam velocity. Then, keeping constant both the beam velocity, at about 30 MeV/u, and the mass of the target, the influence of the beam energy has also been studied by raising the mass of the projectile. The first set of data, from Jahnke et al (1988), presented in Fig.8, shows the weak influence of beam velocity on energy dissipation in the range 27-77 MeV/u. The bump representing the bulk of the most dissipative collisions hardly moves, suggesting some soft saturation effect in the dissipative process. This trend has been confirmed in more exclusive experiments by measuring the characteristics of evaporated charged particles, gated on high neutron multiplicity events. A similar soft saturation has been observed by Jiang et al (1989) in the multiplicity of evaporated light charged particles emitted in coincidence with the neutrons. Moreover, the shape of the energy spectra of backward evaporated particles remain insensitive to the bombarding energy as though the recoil velocity and temperature of their emitting nuclei were only weakly affected by the increase of beam energy. These data are consistent with others, derived by Pochodzalla et al (1987) when measuring the population of widely separated states in complex particles. If the excess of beam energy is not found into an excess of heat, it

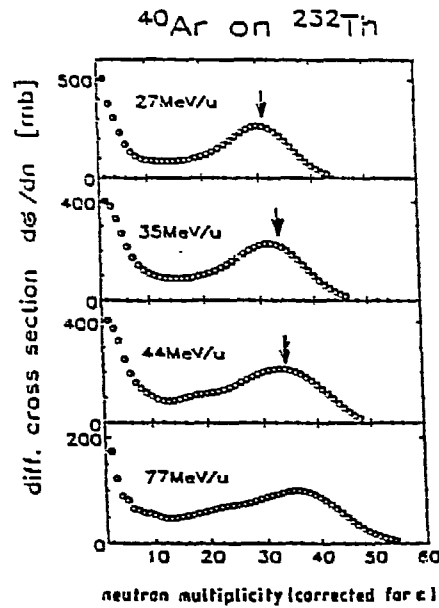


Fig.8 Inclusive neutron multiplicity distributions, measured from several detectors and corrected for detector efficiency for sake of comparison.

must have been evacuated in the first steps of the collision process as a forward jet of non-equilibrated particles. Unfortunately this could not be checked with our experimental set-up.

The main message obtained from this series of measurements is that, increasing the beam velocity above 30 MeV/u does not permit one to increase significantly the thermalized energy. Why is it so in heavy-ion reactions whereas, with light projectiles, energy dissipation seems to still increase with projectiles of higher velocities as shown by Saint-Laurent et al (1982, 1984)? The difference between the two sets of data may stem from the higher temperatures reached in heavy ion collisions. Is there any dynamical limitation due to the similarity between characteristic relaxation time and decay time, both of the order of 10^{-22} s, when T approaches 5 MeV? Is the concept of a thermally equilibrated system still meaningful in such a case?

The second set of data is gathered, in Fig.9, for reactions induced with Ar, Kr and Pb projectiles at 35, 32, 29 MeV/u respectively, on Au and U (or alternatively Th) targets. Beam velocities are quite comparable, whereas masses of considered projectiles vary by a factor of 5. The presented multiplicities are taken at the centroid of the bump in the inclusive neutron multiplicity spectra and corrections have been made for detector efficiencies. These corrections computed with reasonable assumptions, never exceed one third of the given values. Two

interesting features can be noticed. First, neutron multiplicities are systematically larger for the heavier target (Th or U, instead of Au). This can be simply interpreted as an effect of the available energy in the c.m. system. The small reduction observed in the number of evaporated protons, as observed by Jiang et al (1989) and Crema et al (1990), can result from structure effects: due to the difference of N/Z and of Coulomb barrier, charged particles emission is slightly hindered for the heaviest system. The second aspect to be stressed in Fig.9 is the strong increase in neutron multiplicity with the size of the system. If for instance, we compare the two systems Ar+Th and Pb+Au, which present the same neutron to proton ratio, the increase in the number of emitted neutrons (2.5) exceeds considerably the mass ratio (1.5) of the two systems. This is a strong clue that the heavy system is hotter than the light one. The second clue is given when considering the reaction products. Whereas for the most dissipative collisions, the Ar+Th interactions lead to production of conventional fission fragments at 35 MeV/u, we have noticed

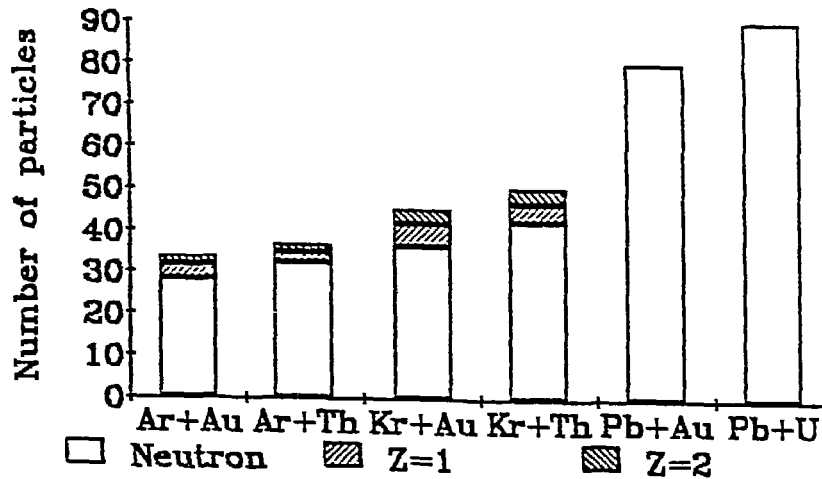


Fig.9 Average multiplicities for evaporated-like light particles, as taken at the centroid of the neutron high multiplicity bump in inclusive data (l.c.p. not yet available for Pb+Au); Data from: 35 MeV/u Ar, 32 MeV/u Kr, 29 MeV/u Pb.

in Sec.2.4 that, in the Pb+Au case, a disassembly in nuclear pieces lighter than fission fragments occurs, as if more energy had been stored into the system.

In summary, the Ar+Au systematics on multiplicities of neutrons and evaporated charged particles has revealed a soft saturation in thermalized energy when increasing the bombarding energy from 27 to 77 MeV/u. On the other hand, when more energy is brought in, by a projectile closer to the target mass at constant velocity of about 30 MeV/u, an important gain in dissipation appears. This gain strongly exceeds the gain of mass of the considered system, thus suggesting that hotter nuclei are formed.

4. FROM PERIPHERAL TO DISSIPATIVE COLLISIONS

From here on, we will focus on reaction mechanisms in considering data for which observables in addition to the neutron multiplicity have been measured. In this exploration we will first look at peripheral collisions and the next chapter will be more specifically devoted to the most dissipative collisions. As will be shown, some peripheral collisions can also be strongly dissipative and there will be some overlap between the present chapter and the next one.

4.1. General features

One way to study peripheral collisions is to set a dedicated silicon telescope close to the grazing angle. An excellent homogeneity and energy resolution of the transmission detector allows simultaneous Z and A identification. An illustration of what has been obtained by Morjean et al (1990) is given, in Fig.10, for ^{41}K produced in the reaction : (27 MeV/u Ar+Au). The narrow peak observed at 1080 MeV can be attributed to one proton pick-up by the ^{40}Ar projectile with a resulting ^{41}K excitation energy below the particle emission threshold. The neutron multiplicity associated with those nuclei of energy larger than 1075 MeV is found to be compatible with zero. This is expected for pick-up reactions where the excitation energy, if any generated in the transfer, is deposited into the receiver, the projectile-like nucleus, and not into the donor, according to Siemens et al (1971). In contrast, the neutron multiplicity averaged over more dissipative reactions is found equal to 1.5. The very high sensitivity of the 4π detector as well as the reliability in the background unfolding procedure can be stressed: no neutrons are observed when they should not be and the onset for their emission is clearly seen. The use of

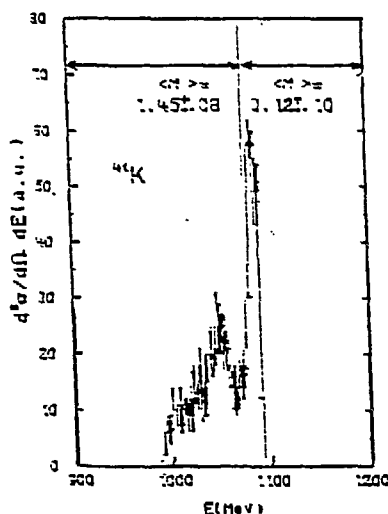


Fig.10 Energy spectrum of ^{41}K at 8° , produced in $^{40}\text{Ar}+\text{Au}$ reactions at 27 MeV/u and associated neutron multiplicities.

such a detector appears very promising for studies, in detail, of the energy sharing between projectile and target in transfer reactions of one or a few nucleons, at intermediate bombarding energies.

The previous type of measurement has been extended to all products detected at 3.7° , i.e. inside the grazing angle for the 44MeV/u Ar+Au reaction. As shown in the contour plot of Fig.11a, giving the yield as a function of both Z and kinetic energy, most of the fragments have kept a velocity close to that of the projectile. The complementary picture (Fig.11b) shows the average neutron multiplicity when exploring the same Z versus E plane as before. For the sake of orientation, the locus of the ridge observed in Fig.11a has been indicated by the dashed line in Fig.11b on top of the neutron multiplicity surface. This allows us to stress the dramatic increase in neutron multiplicity from 0, for $Z=18$, the elastically scattered projectile, to 22 (i.e. close to 30 after efficiency correction) for $Z=3$. At this stage it is worth recalling that the neutron detector is selective in registering with high efficiency the low energy neutrons but presents a very low efficiency for those neutrons that could be emitted by a source at 44 MeV/u. This ensures that most of the detected neutrons come from the target-like nuclei which must be highly excited. What had been called by Borrel et al (1983) or Guerreau et al (1983) a projectile fragmentation process by analogy with the high energy (2.1 GeV/u) process, first observed by

Greiner et al (1975), cannot be interpreted by a simple participant-spectator model. In this model the projectile-like and target-like spectators are left nearly cold. This condition is clearly

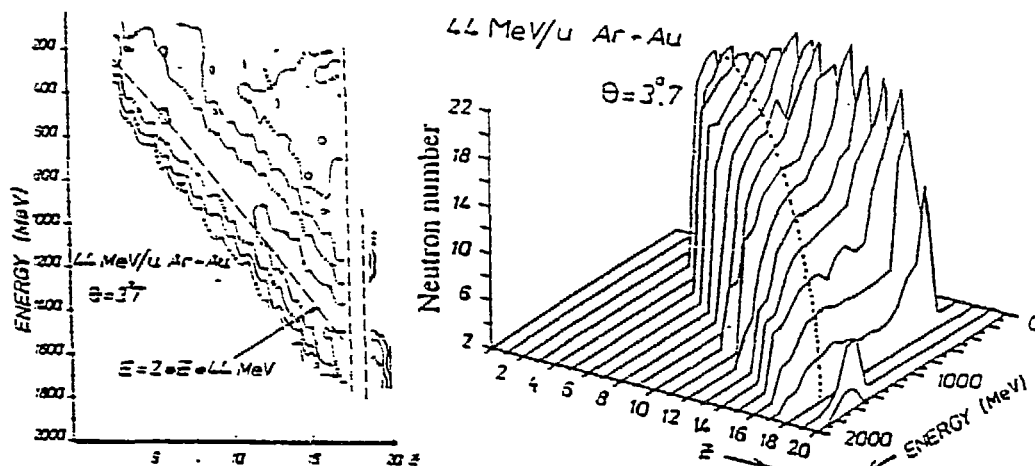


Fig 11 a (left hand side): contours of yields for projectile-like fragments as a function of their atomic number and kinetic energy; b (right hand side): corresponding average neutron multiplicities.

not fulfilled at 44 MeV/u. As discussed in some details by Borderie et al (1990), both one-and-two body dissipation processes have to be taken into account at several tens of MeV/u bombarding energy.

At this stage, we would like to stress that all the considered reactions have to be peripheral for a remaining part of the projectile to survive with nearly projectile velocity. One can conjecture that it is the outer part of the projectile which survives, the part which does not overlap with the target nucleus. As a consequence, the spin imparted to the target-like nucleus should be rather well defined when selected by a coincidence with a well identified projectile-like nucleus. Such reactions could be exploited further in order to generate nuclei with rather well determined charge, mass, excitation energy and spin, whose decay could be studied in detail.

Leaving the ridge of Fig.11a to explore the rest of the map, it can be seen that the projectile-like fragments far from the projectile, either because of their Z or (and) their velocity, are associated with the highest neutron multiplicities: the stronger the damping, the larger the excitation energy of the target-like nucleus appears to be. The continuity showing up in the dissipation process strongly suggests that, even for very dissipative collisions, the observed fragments, or at least part of them, are remnants of the initial projectile. They certainly cannot all be considered as emission, at a preequilibrium stage, of intermediate mass fragments, as observed for example in He induced reaction by Kwiatkowski (1987). As shown in Fig.12, at a slightly different angle than before, and as measured with a less efficient neutron detector _this explains the observed differences in the neutron multiplicities of Fig.11 b and 12_, all average multiplicities line up on a single curve whatever the considered Z of the detected fragment. The excitation energy of the target-like product thus appears to be strongly connected with the kinetic energy loss of the projectile. A similar behavior has also been found at lower bombarding energies by Olmi et al (1987).

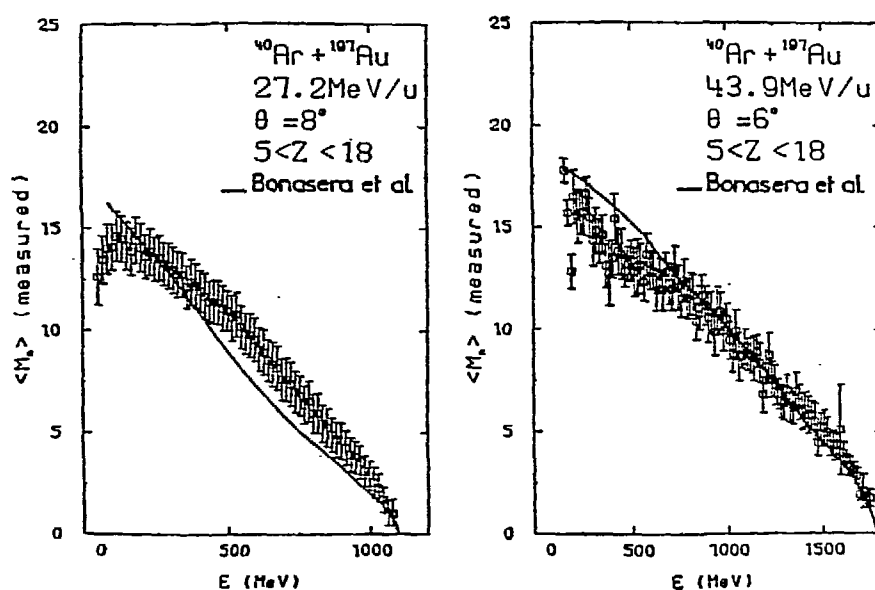


Fig.12 Measured neutron multiplicities as a function of kinetic energy of coincident projectile-like fragments for Ar+Au at two bombarding energies. The data from the model of Bonasera et al (1987), associating one-and-two body dissipation, is given by the solid line.

When the exploration is pushed as far as 20° , a very rapid evolution can be witnessed up to 20° , but beyond, as shown in Fig.13, there is almost no dependence between the measured neutron multiplicity and the nature and energy of the detected products. All reaction channels denote a strong, but similar damping.

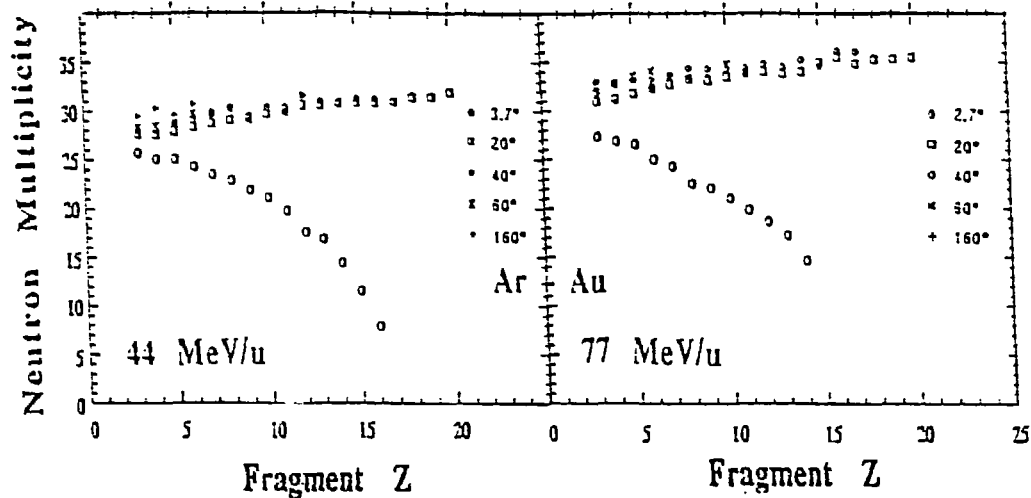


Fig.13 Average neutron multiplicity distributions (efficiency corrected) in coincidence with fragments from the Ar+Au system, at several angles, for two bombarding energies.

In order to get an overview of all data previously shown, we have generated in Fig.14, usual galilean invariant cross section contours as a function of longitudinal and transverse velocities of the fragments. One can recognize a pattern most familiar at lower bombarding energy. As sketched in the right hand part of Fig.14, two branches can be unfolded, which, when overlapping near 0° , generate the somewhat complicated pattern actually measured at small angles. The two distinct components can also be nicely recognized inside the grazing angle (Fig.11a), at least for products close to the projectile mass, with two well different neutron multiplicity characteristics(Fig.11b).

As already noticed by Rivet et al (1988), what is observed at bombarding energies of several tens of MeV/u resembles very closely the well known deep inelastic process and Fig.14 is nothing but a translation of the Wilczynski (1973) picture. The observed fragments are an emanation of the projectile. Sticking time, rotation angle and energy damping depend strongly on the impact parameter as shown by Rivet et al (1988). It is thus a continuous process which

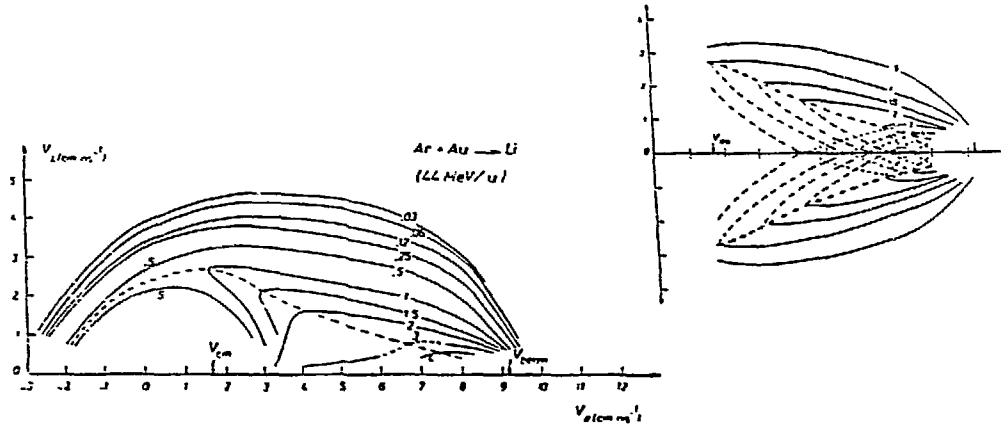


Fig.14 Invariant cross section contours as a function of parallel and transverse velocities for Li produced in Ar+Au reactions at 44 MeV/u.

argues against fitting procedures utilizing three distinct sources, as often done in the past (see for instance Milkau et al 1990). Fig.14 could also be perfectly mocked up using the usual low, intermediate and high velocity sources with ad'hoc parametrization, but without true physical significance.

In summary, the fragments observed close to the grazing angle, with a velocity similar to the beam, do not originate from a process described at higher bombarding energies by a simple participant-spectator picture. This is well demonstrated by the high number of neutrons that can be evaporated by the target-like complementary fragment. At several tens of MeV/u one-body dissipation is still at work that brings high excitation energy into the fragments. The existence of a process much similar to the well known low energy deep inelastic process, showing up in the invariant cross section contour plots, can be confirmed when examining the associated neutron multiplicity patterns. The neutrons bring precise information on the target-like excitation energy. Complementary information from the projectile-like excitation energy, as obtained for instance by Steckmeyer et al (1989) from a dedicated charged particle hodoscope, should permit one to study, in the future, the excitation energy sharing between interacting nuclei. This would be a more direct approach than utilizing kinematic correlations between fragments, as has been done by Dayras et al (1989).

5. HIGHLY DISSIPATIVE COLLISIONS

5.1 Selection of dissipative events

Until recently, selection of dissipative events has been based mainly on the recoil properties of either evaporation residues or, alternatively, on fission products. The larger the dissipated energy, the more recoil the heated system gains. The extreme case would be given by the formation of a true compound nucleus recoiling with the center of mass velocity. When particles are emitted prior to equilibrium or if part only of the system fuses, then, deviation is observed leading to apparent velocities smaller or larger than the center of mass velocity, depending on whether the projectile nucleus is lighter or heavier than the target nucleus. This experimental selection works nicely as long as evaporation residues or binary fission fragments are unique massive fragments in the considered event, with the emission of light particles having only a small distortion effect in slightly broadening the spatial distributions of the heavy nuclei. When the collision gets more violent, the data analysis can become strongly biased by the existence of undetected, extra massive fragments as shown by Fatyga (1987). Therefore, 4π detection of massive fragments would be necessary in order to pursue in a correct manner the recoil measurements.

Instead of measuring heavy fragments over 4π , it can be easier to measure multiplicities of light particles, either charged or neutral. The strong correlation between momentum transfer and energy dissipation, measured through neutron multiplicities, has been firmly established in a number of cases by Galin et al (1988, 1989). As shown for instance in Fig. 15, the multiplicity data appear, in some respects, more reliable than the recoil data: At small fission folding angle, multiplicity remains constant and this reveals simple fluctuations in folding angle, which otherwise could be interpreted as actual 100% momentum transfer. Also, as shown by Schwinn et al (1990), at higher bombarding energies (44, 77 MeV/u), binary fission becomes more and more difficult to disentangle from ternary, quaternary, etc, splittings. The decline of binary fission following high momentum transfer which is observed, has nothing to do with a loss of capacity for energy dissipation. Instead, inclusive neutron multiplicity distributions have revealed (Fig.7) very similar patterns at all incident energies, indicating some soft saturation in the dissipated energy but, by no means, a decline. The use of a multiplicity filter is less restrictive than a kinematic analysis of truncated heavy residues or fission fragment data!

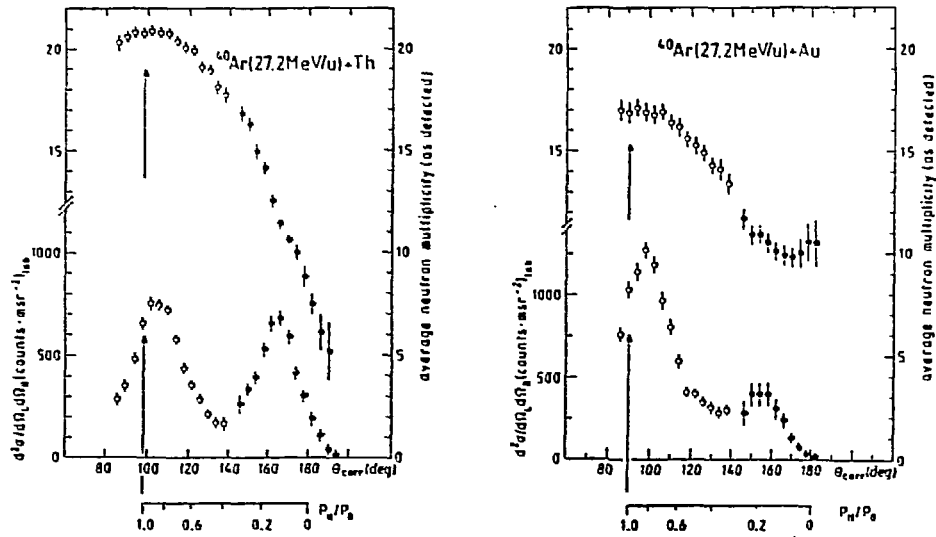


Fig.15 Folding angle distributions for fission fragments produced in the 27 MeV/u Ar+Th and Ar+Au reactions, and associated neutron multiplicities.

5.2 How to infer excitation energy or temperature from measured observables?

The determination of excitation energy from the measured observables requires a model. When recoil properties are measured the model which is usually utilized relies on the massive transfer picture: part of the lighter interacting nucleus fuses with the heavier one at beam velocity. As long as the fusion process is nearly complete, i.e. at bombarding energies up to 30 MeV/u, this model is quite satisfactory. Above, its applicability is more questionable and it probably overestimates the excitation energy. One can also assume that all nucleons participate but with an effective average velocity reduced with respect to the beam velocity. This is probably a better assumption in so far as energy is considered but it clearly overestimates the mass of the excited system. The preequilibrium model of Blann (1985) has also been used, with an arbitrary choice of the exciton numbers (Pollaco 1990).

What can be done when measuring multiplicities of neutrons and sampling evaporated light charged particle measured backward? This approach has been followed by Jiang et al (1989) and by Friedman (1990). It is assumed that all detected neutrons have an evaporative origin,

and this is essentially fulfilled, as shown in Fig.3, because of the natural selectivity of the neutron detector. Moreover, when charged particles are detected at backward angles (in normal kinematics) their evaporative origin is not questionable. However, to integrate over 4π , one needs to know the Jacobian and thus make some assumption on the emitter recoil velocity. Then, two parallel approaches have been followed to determine the excitation energy from the number of evaporated-like particles. On the one hand, Jiang et al (1989) have summed up the energy removed by all particles when emitted in sequence, taking in addition to the separation energy, an average kinetic energy as $2T$ for neutrons and $(B+2T)$ for charged particles, where B and T stand for emission barrier and temperature, respectively. The removed kinetic energy being temperature dependent, one needs to choose a level density parameter and to iterate. The final result is weakly sensitive to the sequence in which charged and neutral particles escape. On the other hand, Friedman (1990) has run the evaporation code he had developed earlier with Lynch (1983), showing that the excitation energy depended critically upon the ratio between

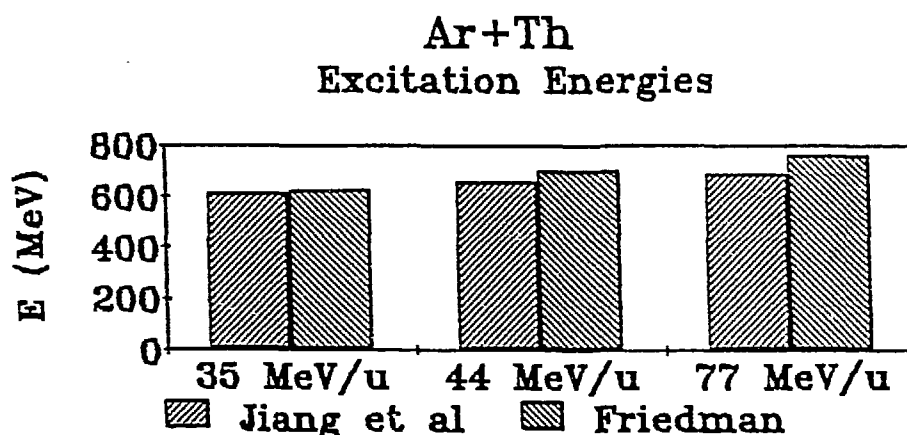


Fig.16 Derivation of excitation energies from evaporated-like neutron and light charged particle multiplicities, following two approaches.

neutron and charged particle multiplicities, but very little on the absolute mass of the considered hot system. As shown in Fig.16, the agreement between the two approaches is quite reasonable, with nevertheless, the first approach leading to a softer saturation than the second.

To conclude this subsection we would like to present, along a similar line as before, data recently obtained by Crema et al (1990) on the 32 MeV/u Kr+Au system. The observables are

the same as previously, i.e. neutron multiplicities and backward evaporated charged particles. but, now, use has been made of the kinematic properties of energy spectra of charged particles to get more precise information. As Crema noticed, in a certain domain, the location of the maximum of these energy spectra depends strongly on the associated neutron multiplicity, as shown in Fig.17. The hotter the emitter, the faster recoiling it is, and the slower the particles

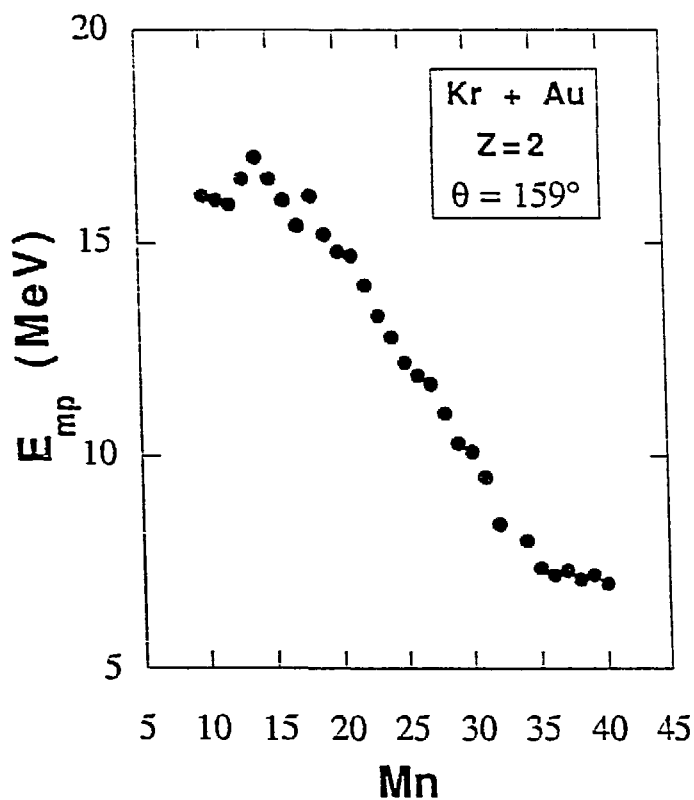


Fig.17 Dependence between neutron multiplicity and location of the maximum of energy spectra for alpha-particles at 159° .

it evaporates backward, appear to be. A simple massive transfer model allows to relate most probable evaporation energy with recoil velocity and, thus, to derive a Jacobian which permits integration over 4π of emitted charged particles(Fig.18). Then, and as done before, but now for different neutron multiplicity bins, excitation energy can be derived by

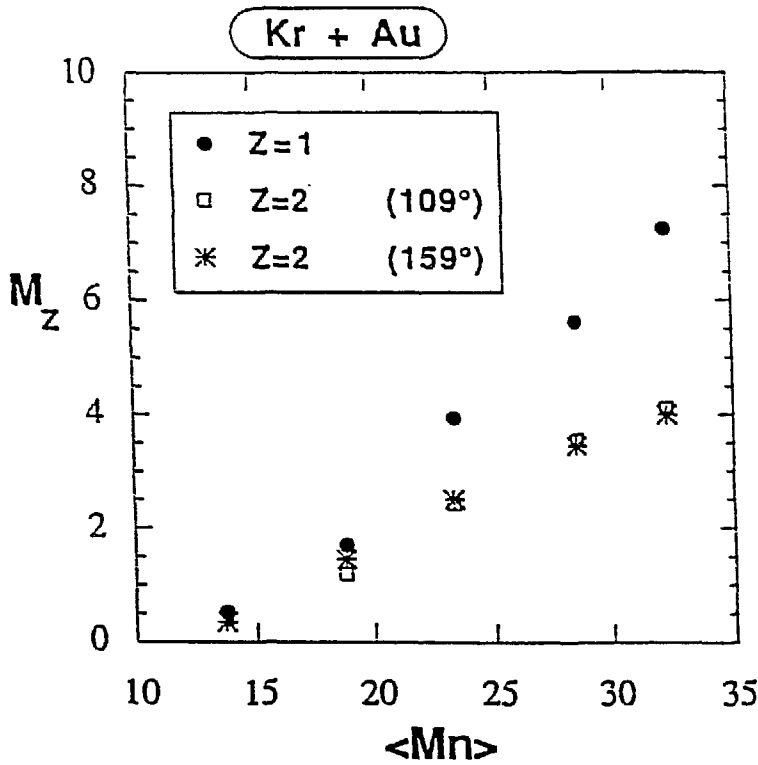


Fig.18 Evaporated-like charged particle multiplicities, integrated over 4π , as a function of measured neutron multiplicities, from data measured at 109° and 159° .

summing up energy removed by both types of particles, neutrons and charged ones. For the highest neutron multiplicity bin (30-34), an excitation energy of 1.2 GeV is derived, i.e. much more than for Ar induced reactions at a similar velocity. Spectral temperatures were also derived, from the slopes of particle energy spectra, as a function of neutron multiplicity. As shown in Fig.19, there is excellent agreement with those derived from excitation energy data, provided a level density parameter of $A/10$ is taken. When presented in the frame of their emitter, the energy spectra show, as a function of the associated neutron multiplicity, a strong evolution in their slopes, and a significant shift in the position of their maximum (Fig.20). Both effects are related to temperature. All these data exhibit a great consistency in the behavior of several

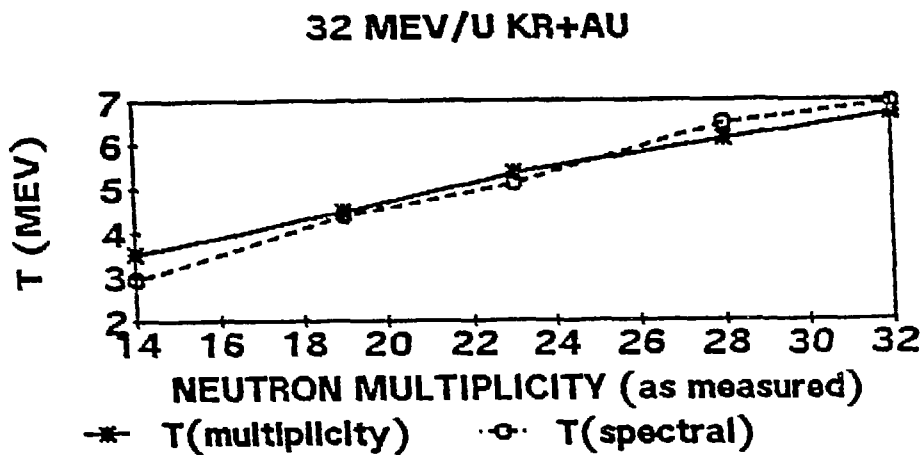


Fig.19 Nuclear temperatures as derived from multiplicity data and spectral slopes (see text).

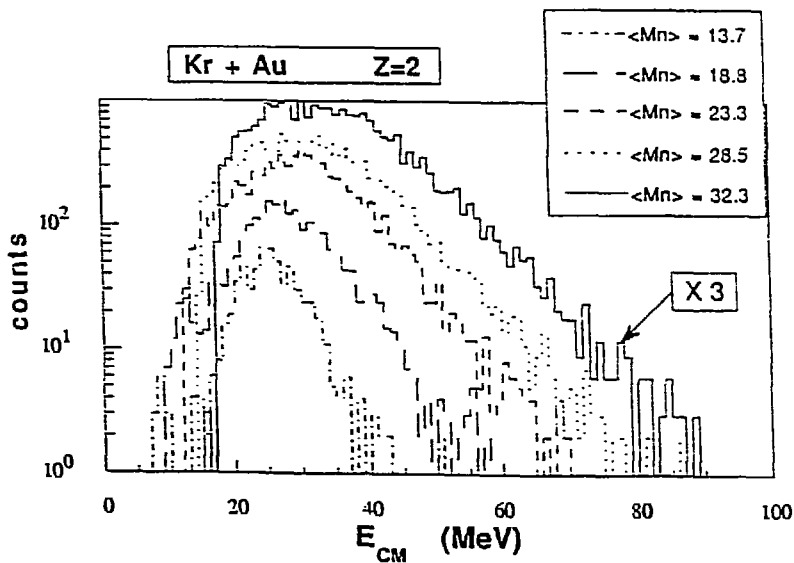


Fig.20 alpha-particle energy spectra, in the reference frame of their emitter, for several neutron multiplicity gates.

weakly dependent observables: neutron and charged particle multiplicities, positions and slopes of charged particle spectra and give very good confidence in the excitation energy (or temperature) values, thus derived.

In these Kr+Au reactions it is thus possible to form nuclear systems in which about 90% of the projectile momentum has been transferred, leading to masses close to 270 and excitation energies of about 1.2 GeV. This represents excitation energies per nucleon unit of 4.5 MeV (or $T=6.7$ MeV, with $a=A/10$). Despite such large amounts of dissipated energy the considered systems appear to behave like any thermally equilibrated nucleus would do at lower temperatures, evaporating a copious number of light particles, isotropically (seen from the neutrons in Fig.3) with typical Maxwellian energy spectra (seen from charged particles). Can such elusive systems be called hot nuclei, or are they blobs of nuclear matter? Dynamic calculations, by Jacquet et al on the Ar+ U system (1990), have shown that the, collective, shape degree of freedom has not enough time to relax before deexcitation starts. Thus, the hot object resembles more a blob of nuclear matter than an idealized nucleus.

5. SUMMARY

We have shown the invaluable benefit that a high efficiency 4π neutron detector can bring to the study of reaction mechanisms following collisions of heavy nuclei at intermediate energy. In addition to global multiplicity, sectorized detectors, such as ORION, furnish gross information on the spatial distribution and hopefully, additional data on their global kinetic energy. Due to the dependence of detection efficiency upon kinetic energy, analysis requires Monte-Carlo simulations for comparison between experimental data and any emission model. Neutron multiplicity has been exploited both as a filter on impact parameter and also to infer excitation energies. Indeed, for heavy nuclei most of the dissipated energy is further removed by neutron evaporation and relatively little by light charged particle emission.

In systematic measurements with projectiles of velocity corresponding to energies between 27 and 77 MeV/u, where both the influence of beam velocity and mass have been investigated separately, it has been shown that the projectile-target mass asymmetry, much more than velocity, has a decisive influence on energy dissipation. The closer the projectile mass to the target mass, the more energy is dissipated per unit mass of the considered projectile plus target system. The latter presents all the characteristics of a thermalized system, evaporating a copious number of light particles: up to about 40 neutrons (after efficiency correction) and 11 light charged particles in the most dissipative collisions between Kr+Au, and 90 neutrons for Pb+U

with a yet unknown number of l.c.p. In the Kr experiment, these particles are isotropically emitted in the frame of a fused system, excited with 1.2 GeV. Moreover, l.c.p. exhibit Maxwellian energy distributions as in any standard evaporation process. We are now eager to better characterize the properties of the Pb+Au(U) systems for which about 1/3 of the neutrons are freed in a rather large fraction of all collisions. The thermalized energy should then approach very closely the total binding energy of the two interacting nuclei.

ACKNOWLEDGMENTS

The experimental program with 4π neutron detectors has been initiated at GANIL in 1986. Since then, five experiments have been run, with three different detectors from CE Bruyères-le-Châtel, HMI Berlin, GANIL. It is a pleasure to thank the numerous colleagues who have taken part in any stage of this program and especially those involved in all experiments: D Guerreau, D Jacquet, U Jahnke, B Lott, M Morjean and J Pouthas. I am grateful to S Bresson, E Crema and E Piasecki for rapid evaluation of most recent Kr and Pb data and to D Horn and E Piasecki for a careful reading of the manuscript.

REFERENCES

- Blann M 1985 *Phys. Rev.* C31 1245
- Bonasera A, Di Toro M, Grégoire C 1987 *Nucl. Phys.* A463 653
- Bonche P, Levit S, Vautherin D *Nucl. Phys.* 1984 A427 278 and 1985 A436 265
- Borderie B, Rivet M F, Tassan-Got L 1990 *Orsay Preprint IPNO-DRE-90-06* to appear in *Ann. Phys. Fr*
- Borrel V, Guerreau D, Galin J, Gatty B, Tarrago X 1983 *Phys. Lett.* 131B 293
- Bougault R, Delaunay F, Genoux-Lubain A, Le Brun C, Lecolley J F, Lefebvres F, Louvel M, Steckmeyer J C, Adloff J C, Bilwes B, Bilves R, Glaser M, Rudolf G, Scheibling F, Stugge L, Ferrero J L 1990 *Bormio Winter Meeting and LPC Preprint LPCC 90-02*
- Brack M, Quentin P 1974 *Physica Scripta* A10 163
- Cheifetz E, Jared D, Giustie R, Thompson S G 1972 *Phys. Rev.* C6 1348
- Crema E, Galin J, Gatty B, Guerreau D, Guilbault F, Jacquet D, Jahnke U, Jiang D X, Lebrun C, Lott B, Morjean M, Piasecki E, Pouthas J, Saint-Laurent F, Schwinn E, Wang X M, *to be published*
- Dayras R, Coniglione R, Barrette J, Berthier B, De Castro Rizzo D M, Cisse O, Gadi F, Legrain R, Mermaz M C, Delagrangé H, Mittig W, Heusch B, Lanzano G, Pagano A 1989 *Phys. Rev. Lett.* 62 1013
- Delagrangé H, Grégoire C, Scheuter F, Abe Y 1986 *Z. Phys.* A323 437
- Fatyga M, Kwiatkowski K, Viola V E, Wilson W G, Tsang M B, Pochodzalla J, Lynch W, Gelbke C K, Fields D J, Chitwood C B, Chen Z, Nayak T 1987 *Phys. Rev. Lett.* 58 2527

Frehaut J 1976 *Nucl. Inst. Meth.* 135 511

Friedman W A 1990 *Univ. Madison Preprint Mad/NT/90-08*

Friedman W A, Lynch W G 1993 *Phys. Rev.* C28 16

Galin J, Ingold G, Jahnke U, Hilscher D, Lehmann M, Rössner H, Schwinn 1988, *Z. Phys.* 331 63

Galin J, Wang X M, Grima E, Guerreau D, Jiang D X, Morjean M, Pouthas J, Saint-Laurent F, Sokolov A, Gatty B, Jasquet D, Lott B, Jahnke U, Schwinn E, Piasecki E, Charvet J L 1990 *GANIL-Preprint 90 09*, and *World Scientific Symp. on heavy ion collisions Obernai-France* Ed by B Heusch and M Ishihara

Guerreau D, Borrel V, Jasquet D, Galin J, Gatty B, Tarraga X 1993 *Z. Phys.* A314 191

Greiner D E, Linstrom P J, Heckmann H H, Cork B, Bieser F S, 1975 *Phys. Rev. Lett.* 35 152

Jasquet D, Peaslee G F, Alexander J M, Borderie B, Duck E, Galin J, Gardes D, Grégoire C, Fuchs H, Lefort M, Rivet M F, Tarraga X 1990 *Nucl. Phys.* A511 195

Jahnke U, Ingold G, Hilscher D, Ort H, Kopp E A, Feige G, Brandt R 1983 *Lecture Notes in Physics* (Springer-Berlin) 176 179

Jahnke U 1988 *XXth Mikolajki Summer School*

Jiang D X, Doubre H, Galin J, Guerreau D, Piasecki E, Gramer B, Ingold G, Jahnke U, Schwinn E, Charvet J L, Frehaut J, Lott B, Magnago G, Morjean M, Patin Y, Pranal Y, Uzureau J L, Gatty B, Jasquet D 1990 *Nucl. Phys.* A593 569

Kwiatkowski K, Bastkin J, Karkowski H, Fatyga M, Viola V E 1986 *Phys. Lett.* B171 41

Milkau U, Berdermann, Berthier B, Bouissou P, Cerruti G, Demeyer A, Eckert E M, Guinet D, Hildenbrand K D, Hübele J, Imme G, Kreuz P, Kunde G J, Leray S, Lhensret P, Lucas R, Lynen U, Mazur G, Müller W F J, Ngô C, Pirkenburg G H, Pechodzalla J, Rabe H J, Rasiti G, Ribrag M, Sann H, Stetzer H, Tomasi E, Trautmann W, Trostel R, Wada R 1990 *GSI Preprint GSI-90-14*

Morjean M, Doubre H, Galin J, Guerreau D, Jiang D X, Pouthas J, Charvet J L, Frehaut J, B Lott, Magnago G, Patin Y, Pranal Y, Jasquet D, Ingold G, Jahnke U 1990 *GANIL Preprint 90 and submitted to Nucl. Phys.*

Nemeth J, Barranco M, Ngo C, Tomasi E 1986 *Z. Phys.* A223 419

Orni A 1987 *Nucl. Phys.* A471 976

Piasecki E, Bougault R, Bresson S, Collin J, Grima E, Galin J, Gatty B, Genoux-Lubin A, Guerreau D, Horn D, Jastrzebski J, Jasquet D, Jahnke U, Kerdyasz A, Le Brun G, Lesotley J F, Lott B, Louvet M, Morjean M, Paulot C, Pionkowski L, Pouthas J, Quednau B, Schroeder W U, Schwinn E, Skulski W, Töke J to be published

Pechodzalla J, Selske K, Lynch W G, Maier M, Arduin D, Delagrange H, Doubre H, Grégoire C, Kwasowski A, Mittag W, Peghaire A, Péter J, Saint-Laurent F, Zwieglini B, Bizard G, Lefebvres F, Tamain B, Québert J, Vinyo Y P, Friedman W A, Beal D H 1987 *Phys. Rev.* C35 1685

Peitsch J, Signarbieux G 1974 *Nucl. Inst. Meth.* 114 119

Pollaco E G, Volant G, Cassagneu Y, Genjeaud M, Dayras R, Harar S, Legrain R, Sauvestre J E 1990 *Saclay-Preprint DPh-N/92589*

Pist N, Wang X M unpublished

Raines F 1954 *Rev. Sci. Inst.* 25 1661

Rivet M F, Borderie B, Grégoire G, Jouan D, Remaud B 1988 *Phys. Lett.* 215B 55

Saint-Laurent F, Conjeaud M, Dayras R, Harar S, Oeschler H, Volant C *Phys. Lett.* 1982 110B 372 and 1984 *Nucl. Phys.* A422 307

Schroeder W U 1988 *Proc. of the Symposium on Nuclear Physics Bombay. Indian AEC* 31A 231
Schwinn E et al *to be published*

Siemens P J, Bondorf J P, Gross D H E, Dickmann F 1971 *Phys. Lett.* 36B 24

Sokolov A 1990 *Ph.D. Thesis, GANIL and to be published*

Steckmeyer J C, Bizard G, Brou R, Eudes P, Laville J L, Natowitz J B, Patry J P, Tamain B, Tiphagne A, Doubre H, Pégahaire A, Péter J, Rosato E, Adloff J C, Kamili A, Rudolf G, Scheibling F, Guibault F, Lebrun C, Hanappe F 1989 *Nucl. Phys.* A500 372

Suraud E 1987 *Nucl. Phys.* A462 109

Vautherin D, Treiner J, Veneroni M 1987 *Phys. Lett.* B191

Vinet L, Sebille F, Grégoire C, Remaud B, Schuck P 1986 *Phys. Lett.* B172 17 and 1987 *Nucl. Phys.* A468 321

Wilczynski J 1973 *Phys. Lett.* 47B 484

Wilcke W W, Birkelund J R, Wollersheim H J, Hoover A D, Huizenga J R, Schroeder W U, Tubbs L E 1980 *Atomic Data and Nuclear Data Tables* 25 389